

# Diffractive dijet production at CDF

Konstantin Goulios  
(for the CDF Collaboration)

*The Rockefeller University, 1230 York Avenue, New York, NY 10065, USA*

**Abstract.** We present a CDF measurement of diffractive dijet production in  $\bar{p}p$  collisions at 1.96 TeV at the Fermilab Tevatron Collider using data from an integrated luminosity of  $\approx 310 \text{ pb}^{-1}$  collected by triggering on a high transverse momentum jet in coincidence with a recoil antiproton detected in a roman pot spectrometer. We report final results for 4-momentum transfer squared  $t > -4 \text{ GeV}^2$ , antiproton-momentum-loss fraction within 0.03-0.09, Bjorken- $x$  of the interacting parton in the antiproton in the range 0.001-0.1, and jet transverse energies from 10 to 100 GeV.

**Keywords:** diffraction, pomeron, total cross section

**PACS:** 13.85.Lg, 13.85.Dz, 13.87.Ce, 12.40.Nn

## 1. INTRODUCTION

We present final results from a CDF measurement of single-diffractive (SD) dijet production in  $\bar{p}p$  collisions at  $\sqrt{s} = 1.96 \text{ TeV}$  at the Fermilab Tevatron Collider using data collected by triggering on a high transverse momentum jet in coincidence with a recoil antiproton detected in a Roman Pot Spectrometer (RPS) [1]. We consider proton diffractive dissociation,  $\bar{p} + p \rightarrow \bar{p} + G_{\bar{p}} + X_p$ , characterized by a rapidity gap (region of pseudorapidity <sup>1</sup> devoid of particles) adjacent to an escaping  $\bar{p}$ , and a final state  $X_p$  representing particles from the dissociation of the proton [2]. The rapidity gap, presumed to be caused by a color-singlet exchange with vacuum quantum numbers between the  $\bar{p}$  and the dissociated proton, traditionally referred to as Pomeron ( $P$ ) exchange, is related to  $\xi_{\bar{p}}$ , the forward momentum loss of the surviving  $\bar{p}$ , by  $G_{\bar{p}} = -\ln \xi_{\bar{p}}$ .

Several diffractive dijet results were obtained by CDF in Run I [3]-[6]. Among these, most striking is the observation of a breakdown of QCD factorization, expressed as a suppression by a factor of  $\mathcal{O}(10)$  of the diffractive structure function (DSF) measured in dijet production relative to that derived from fits to parton densities measured in diffractive deep inelastic scattering (DDIS) at the DESY  $e-p$  collider HERA (see [5]).

The present Run II diffractive dijet measurement was performed in order to further characterize the diffractive structure function by measuring  $t_{\bar{p}}$  distributions over a wide range of  $t$  and jet transverse energy,  $E_T^{\text{jet}}$ , namely  $-t_{\bar{p}} \leq 4 \text{ GeV}^2$  and  $10^2 < Q^2 \approx (E_T^{\text{jet}})^2 < 10^4 \text{ GeV}^2$ , and to search for diffractive dips. Below, we present the main results of this measurement and compare them with theoretical expectations.

---

<sup>1</sup> Rapidity,  $y = \frac{1}{2} \ln \frac{E+p_L}{E-p_L}$ , and pseudorapidity,  $\eta = -\ln \tan \frac{\theta}{2}$ , where  $\theta$  is the polar angle of a particle with respect to the proton beam ( $+\hat{z}$  direction), are used interchangeably for particles detected in the calorimeters, since in the kinematic range of interest in this analysis they are approximately equal.

## 2. MEASUREMENT

*Detector.* Figure 1 is a schematic plan view of the detector used in this measurement, showing the main CDF II central detector and the forward detector-components essential to this measurement. The forward components include a Roman Pot Spectrometer (RPS), which measures  $\xi_{\bar{p}}$  and  $t_{\bar{p}}$  with resolutions  $\delta\xi_{\bar{p}} = 0.001$  and  $\delta t_{\bar{p}} = \pm 0.07 \text{ GeV}^2$  at  $\langle -t_{\bar{p}} \rangle \approx 0.05 \text{ GeV}^2$ , where  $\delta t_{\bar{p}}$  increases with  $t_{\bar{p}}$  with a  $\propto \sqrt{-t_{\bar{p}}}$  dependence.

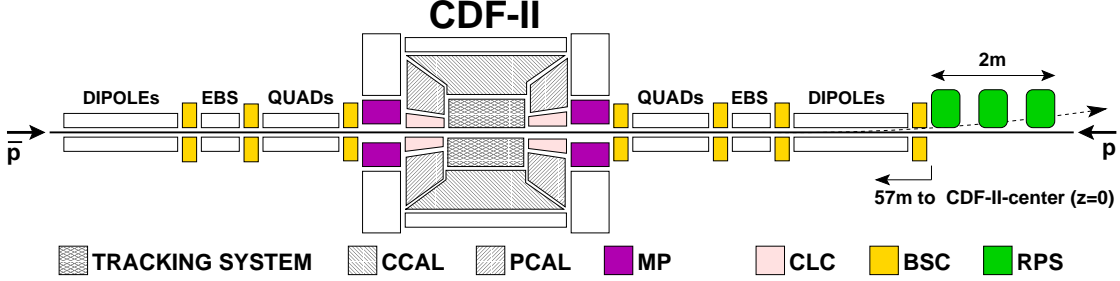


**FIGURE 1.** Schematic plan view of the detector, showing the main detector (CDF II) with tracking system and calorimeters (central, CCAL; plug, PCAL), and forward components (Cerenkov Luminosity Counters, CLC; MiniPlugs, MP; Roman Pot Spectrometer, RPS). EBS are electrostatic beam separators.

*Data samples.* This analysis is based on data corresponding to an integrated luminosity of  $\mathcal{L} \approx 310 \text{ pb}^{-1}$  collected in 2002–2003. Events were selected online with a three-level prescaled triggering system accepting RPS-triggered inclusive and jet-enriched events by requiring at least one calorimeter tower with  $E_T > 5, 20, \text{ or } 50 \text{ GeV}$  within  $|\eta| < 3.5$ . Jets were reconstructed using the midpoint algorithm [7].

The majority of the data used in this analysis were recorded without RPS tracking information. For these data, the value of  $\xi_{\bar{p}}$  was evaluated from calorimeter information and is designated as  $\xi_{\bar{p}}^{CAL}$ . The  $\xi_{\bar{p}}^{CAL}$  was then calibrated against  $\xi$  obtained from the RPS,  $\xi_{\bar{p}}^{RPS}$ , using data from runs in which RPS tracking was available.

The following trigger definitions are used for these measurements:

- RPS: RPS trigger counters in time with a  $\bar{p}$  crossing the nominal interaction point;
- J5 (J20, J50): jet with  $E_T^{jet} \geq 5$  (20, 50) GeV in CCAL or PCAL;
- RPS·Jet5 (Jet20, Jet50): RPS trigger in coincidence with J5 (J20, J50).

## 3. RESULTS

Figure 2 shows kinematic distributions for SD and ND events. On (*left*), the average  $\eta$  of the two highest  $E_T$  jets in the event,  $\eta^*$ , is seen to be centered for ND while shifted to a higher value for SD events; on (*right*), the average particle multiplicity in the MiniPlug,  $M_{\bar{p}}$ , is  $\sim 9$  for ND and peaks at zero for SD events. These results are in agreement with expectations from the presence of a rapidity gap adjacent to the outgoing  $\bar{p}$  in SD events.

In Fig. 3, we compare on (*left*) the mean dijet transverse energy between SD and ND events, and on (*right*) the  $x_{BJ}$  (Bjorken- $x$ ) distribution of the ratio of (SD/ $\Delta\xi$ )/ND event-

rates for various values of  $\langle Q^2 \rangle \approx \langle E_T^* \rangle^2$  over a range of two orders of magnitude. These plots show that the SD and ND distributions are very similar.

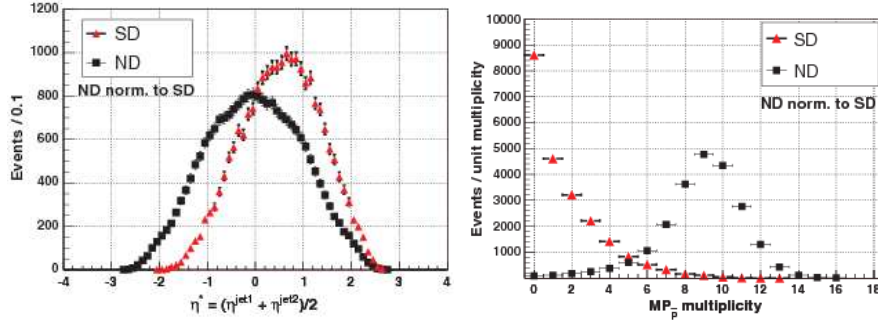


**FIGURE 2.** Distributions for SD and ND events: (left) average  $\eta$  distribution of the two highest  $E_T$  jets; (right) multiplicity distributions in the  $MP_{\bar{p}}$  calorimeter.

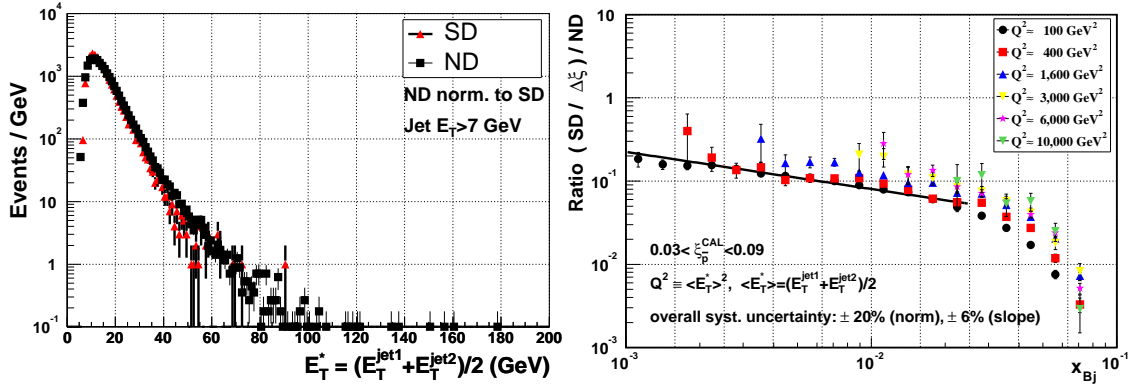


**FIGURE 3.** (left) Mean dijet transverse energy for SD and ND events normalized to the SD events; (right) ratios of SD to ND dijet-event rates vs  $x_{Bj}$  for various values of  $\langle Q^2 \rangle \approx \langle E_T^* \rangle^2$ .

The  $t$  distributions for RPS inclusive and various dijet event samples are shown in Fig. 4 for  $-t < 1 \text{ GeV}^2$  fitted to two exponential terms, and in Fig. 5 for  $-t < 4 \text{ GeV}^2$ . No significant variations are observed over a wide range of  $\langle Q^2 \rangle$ . For  $-t < 0.5 \text{ GeV}^2$  all  $t$  distributions, both for the inclusive and the high  $\langle Q^2 \rangle$  samples, are compatible with the expectation from the “soft” Donnachie-Landshoff (DL) model [8]. The rather flat  $t$  distributions at large  $-t$  shown in Fig. 5 are compatible with a possible existence of an underlying diffraction minimum around  $-t \sim 2.5 \text{ GeV}^2$  filled by  $t$ -resolution effects.

The above results favor models of hard diffractive production in which the hard scattering is controlled by the parton-distribution-function of the recoil antiproton while the rapidity-gap formation is governed by a color-neutral soft exchange [9]-[12].

## ACKNOWLEDGMENTS

I would like to thank Michele Gallinaro, Koji Terashi, Mary Convery, and Christina Mesropian for invaluable contributions, my colleagues at the CDF Collaboration, and

the Office of Science of the Department of Energy for its generous financial support.

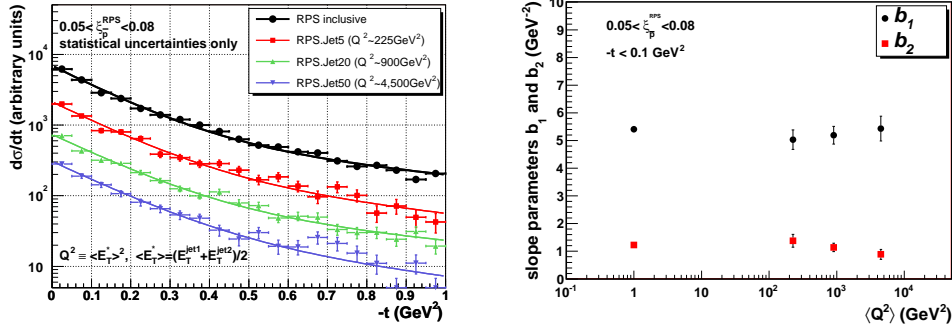


**FIGURE 4.** (left)  $t_{\bar{p}}$  distributions for SD RPS data of various  $\langle Q^2 \rangle$  values within  $0.05 < \xi_{\bar{p}}^{\text{RPS}} < 0.08$ ; (right) slope parameters  $b_1$  and  $b_2$  vs  $\langle Q^2 \rangle$  of a fit to  $dN_{\text{events}}/dt = N_{\text{norm}}(A_1 e^{b_1 t} + A_2 e^{b_2 t})$  with  $A_2/A_1 = 0.11$  (average over all data subsamples). The RPS-inclusive points are arbitrarily placed at  $\langle Q^2 \rangle = 1 \text{ GeV}^2$ .

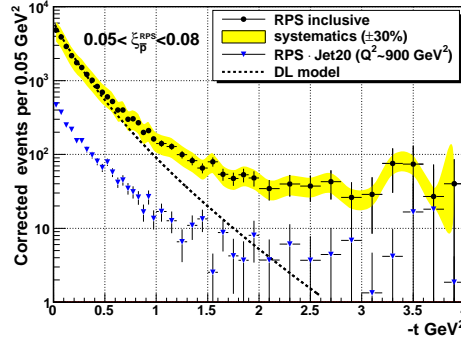


**FIGURE 5.**  $t$  distributions of two SD event samples for  $0.05 < \xi_{\bar{p}}^{\text{RPS}} < 0.08$  corrected for RPS acceptance after background subtraction: RPS inclusive, for which  $\langle Q^2 \rangle \simeq 1 \text{ GeV}^2$  (circles), and  $\langle Q^2 \rangle \simeq 900 \text{ GeV}^2$  events (triangles); the curve is the expectation of the Donnachie-Landshoff (DL) model [8] normalized to the RPS inclusive data within the region of  $-t < 0.5 \text{ GeV}^2$ .

## REFERENCES

1. T. Aaltonen *et al.* (CDF Collaboration), Phys. Rev. D **86**, 032009 (2012); arXiv:1206.3955 [hep-ex].
2. V. Barone and E. Predazzi, “High-Energy Particle Diffraction”, Springer Press, Berlin (2002).
3. F. Abe *et al.*, (CDF Collaboration), Phys. Rev. Lett. **74**, 855 (1995).
4. F. Abe *et al.* (CDF Collaboration), Phys. Rev. Lett. **79**, 2636 (1997).
5. T. Affolder *et al.* (CDF Collaboration), Phys. Rev. Lett. **84**, 5043 (2000).
6. D. Acosta *et al.* (CDF Collaboration), Phys. Rev. Lett. **88**, 151802-(1-6) (2002).
7. G. C. Blazey *et al.*, “Run II Jet Physics”, in *Proceedings of the Run II QCD and Weak Boson Physics Workshop*; arXiv:hep-ex/0005012 (2000).
8. A. Donnachie and P. Landshoff, Phys. Lett. **B518**, 63 (2001).
9. K. Goulianos, “Renormalized Diffractive Parton Densities,” in *Diffraction 06, International Workshop on Diffraction in High-Energy Physics*, Adamantas, Milos island, Greece (2006), PoS (DIFF2006) 044.
10. S. J. Brodsky *et al.*, Phys. Rev. D **71**, 074020 (2005).
11. A. B. Kaidalov *et al.*, Eur. Phys. J. C **21**, 521 (2001).
12. B.Z. Kopeliovic *et al.*, Phys. Rev. D **76**, 034019 (2007).